Chemistry & Biology, Vol. 12, 797–809, July, 2005, ©2005 Elsevier Ltd All rights reserved. DOI 10.1016/j.chembiol.2005.05.010

Inhibition of hIAPP Amyloid-Fibril Formation and Apoptotic Cell Death by a Designed hIAPP Amyloid-Core-Containing Hexapeptide

Marianna Tatarek-Nossol,[1,3] Li-Mei Yan,[1,3] Anke Schmauder,[1] Konstantinos Tenidis,[1] Gunilla Westermark,[2] and Aphrodite Kapurniotu[1,*]
[1]Laboratory of Bioorganic and Medicinal Chemistry
Institute of Biochemistry
University Hospital of the Rheinisch-Westfälische Technische Hochschule Aachen
D-52074 Aachen
Germany
[2]Department of Biomedicine and Surgery
Cell Biology
Linköping University
SE-58185 Linköping
Sweden

Summary

The pathogenesis of type II diabetes is associated with the aggregation of the 37-residue human islet amyloid polypeptide (hIAPP) into cytotoxic β sheet aggregates and fibrils. We have recently shown that introduction of two N-methyl rests in the β sheet- and amyloid-core-containing sequence hIAPP(22–27), or NFGAIL converted this amyloidogenic and cytotoxic sequence into nonamyloidogenic and noncytotoxic NF(N-Me)GA(N-Me)IL. Here, we show that NF(N-Me)GA(N-Me)IL is able to bind with high-affinity full-length hIAPP and to inhibit its fibrillogenesis. NF(N-Me)GA(N-Me)IL also inhibits hIAPP-mediated apoptotic β cell death. By contrast, unmodified NFGAIL does not inhibit hIAPP amyloidogenesis and cytotoxicity, suggesting that N-methylation conferred on NFGAIL the properties of NF(N-Me)GA(N-Me)IL. These results support the concept that rational N-methylation of hIAPP amyloid-core sequences may be a valuable strategy to design pancreatic-amyloid diagnostics and therapeutics for type II diabetes.

Introduction

Type II diabetes is a pancreatic β cell-degenerative disease that today affects about 200 million people worldwide and leads, through progressively increasing peripheral insulin resistance and decline of β cell function, to a severe deterioration of the physiological functions that are under glycemic control and to a number of micro- and macrovascular complications [1, 2]. A characteristic pathophysiological feature of more than 95% of the type II diabetics is the formation of amyloid deposits in the pancreas [1, 3].

Pancreatic-amyloid deposits in humans consist mainly of β sheet fibrillar aggregates of the 37-residue polypeptide human islet amyloid polypeptide (hIAPP) (Figure 1A) [4]. hIAPP is expressed in the β cells, and in its soluble form, it is believed to play an important role in glucose homeostasis, most likely as an insulin counter-regulator [5, 6]. Insoluble hIAPP amyloid aggregates, however, colocalize with degenerated β cells, and their formation is linked to the progressive deterioration of β cells and type II diabetes pathogenesis [1, 3, 7]. In addition, soluble oligo- and multimeric hIAPP amyloid aggregates have been suggested to be cytotoxic [8–11]. Although both the self-assembly state and the morphological features of the cytotoxicity-mediating hIAPP species are yet to be identified, substantial amount of evidence suggests that these species may form within the pathway of hIAPP amyloid fomation [8–12]. The latter one is a not yet fully understood, multistep nucleation- and concentration-dependent process that proceeds via a conformational transition of mainly random coil hIAPP into β sheet-containing amyloid aggregates [11, 13, 14]. In addition, there is a clear species and sequence specificity of the amyloidogenic potential of the hIAPP sequence [8]. For example, the rat hIAPP sequence (rIAPP) differs in 6 out of 37 residues from the human one and is not capable of forming amyloid fibrils.

To date, two classes of inhibitors of hIAPP amyloidogenicity and/or cytotoxicity have been described. The first one includes aromatic organic compounds such as Congo red, rifampicin, and others that bind to amyloid fibrils and/or suppress amyloid-fibril formation [15–19]. Some of the compounds have been reported also to inhibit hIAPP cytotoxicity and to inhibit amyloidogenicity and/or cytotoxicity by other amyloid peptides [16, 18, 19]. The second class of inhibitors consists of short synthetic peptides that have been derived from hIAPP sequences that contain hIAPP self-recognition domains. These inhibitors are short partial hIAPP sequences in a nonmodified form, i.e., hIAPP(20–25) and hIAPP(24–29) [20], whereas very recently, short hIAPP self-recognition sequences carrying α-aminoisobutyric acid (Aib) have also been reported to inhibit hIAPP amyloid formation [21]. However, although some of the above peptides have been shown to be able to inhibit hIAPP amyloidogenesis, to date, only one of them, hIAPP(20–25), has been reported to be capable of reducing both hIAPP amyloid formation and cytotoxicity [20]. Therefore, rationally designed compounds that may be able to interfere with the amyloid-fibril formation pathway of hIAPP and affect both hIAPP fibril formation and related cytotoxicity are important tools for both understanding the mechanism of hIAPP-amyloidogenesis-related cytotoxicity and developing novel molecular strategies for the treatment of type II diabetes.

We have recently applied a chemical strategy to convert short, amyloidogenic, and cytotoxic hIAPP sequences into highly soluble, nonamyloidogenic, and noncytotoxic ones [22]. This has been achieved via the introduction of conformational constraints in form of N-methylation of two selected amide bonds within short hIAPP sequences containing an hIAPP "amyloid-core" region. The strategy of N-methylation of peptide

*Correspondence: akapurniotu@ukaachen.de
[3]These authors contributed equally to this work.

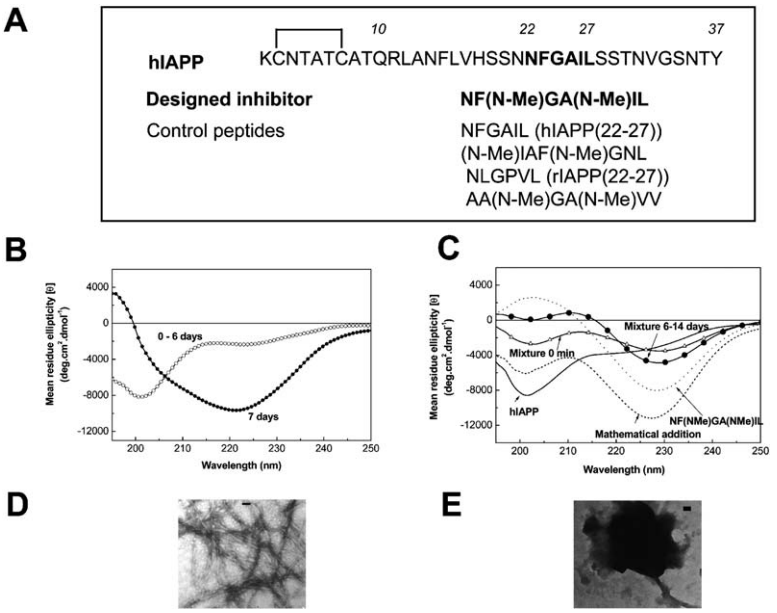

Figure 1. Primary Structures of Peptides Used in This Study and Inhibition of hIAPP β Sheet Formation and Fibrillogenesis by the Designed Inhibitor as Studied by CD and EM

(A) Scheme showing the primary structure of hIAPP, the designed N-methylated hexapeptide (in bold), and various control peptides. The residues of the hIAPP amyloid-core region hIAPP(22–27) are shown in bold. The one-letter code is used for the amino acids. hIAPP contains an amide at the C terminus, whereas the other sequences are peptide acids.

(B–E) Interaction of NF(N-Me)GA(N-Me)IL with hIAPP and its inhibitory effect on hIAPP aggregation into β sheets and amyloid-fibril formation as assessed by CD (B and C) and EM (D and E). (B) CD spectra of hIAPP alone (5 μM) at various time points of the incubation show that the conformational transition into aggregated β sheets and insolubilization are accomplished at about 7 days after the beginning of the incubation. (C) CD spectrum of the mixture of hIAPP (5 μM) with NF(N-Me)GA(N-Me)IL (50 μM) at time 0 min and a representative spectrum for the time period 6–14 days are shown. For comparison, the spectra of hIAPP and of NF(N-Me)GA(N-Me)IL alone and also the mathematical addition of the hIAPP and NF(N-Me)GA(N-Me)IL spectra (at 0 min) are shown. (D) Representative electron micrograph of the hIAPP solution of the CD experiment of (B) (hIAPP alone) after incubation for 7 days and appearance of insoluble aggregates. (E) Representative electron micrograph of the solution of the CD experiment showed in (C) (hIAPP with NF[N-Me]GA[N-Me]IL) after incubation for 14 days. Bars in the electron micrographs represent 100 nm.

amide bonds has been a well-known protein-design approach to suppress the H-bonding ability of an NH group and to restrict the conformation of the backbone [23–26]. Also, recently, studies on the applicability of N-methylated sequences of the Alzheimer's peptide β-amyloid peptide (Aβ) for inhibition of Aβ amyloid formation have been reported [27, 28]. According to our design approach, short hIAPP amyloid-core-containing sequences that have been double N-methylated on the one side of the β strand should be able to interact with their amyloid-forming precursor sequences and possibly inhibit amyloid formation and cytotoxicity [22]. One of the hIAPP amyloid-core sequences that we modified was the hexapeptide hIAPP(22–27) or NFGAIL (Figure 1A). NFGAIL has been previously identified as a short hIAPP "amyloid-core"-containing sequence that is able to self-associate into β sheets and cytotoxic amyloid fibrils [29–31]. Based on an NMR-derived model of pancreatic amyloid, N-methylations were introduced at Gly24 and Ile26, and we devised NF(N-Me)GA(N-Me)IL (Figure 1A) [22, 32]. In fact, NF(N-Me)GA(N-Me)IL was found to be highly soluble, unable to aggregate into β sheets and cytotoxic amyloid, and inhibited amyloid formation by its precursor hexapeptide NFGAIL [22]. Based on these results and the hypothesis that NFGAIL might represent a crucial self-recognition and amyloid-core sequence of full-length hIAPP, NF(N-Me)GA(N-Me)IL appeared to be a promising candidate for inhibition of amyloid-fibril formation and cytotoxicity of hIAPP [29–32].

Here, we present biophysical and biochemical studies on the interaction of NF(N-Me)GA(N-Me)IL with hIAPP and its effect on hIAPP amyloid-fibril formation and cytotoxicity. The interaction of NF(N-Me)GA(N-Me)IL with hIAPP and its effects on hIAPP conformation and aggregation into β sheets and amyloid fibrils were studied by far-UV circular dichroism spectroscopy (CD), electron microscopy (EM), fluorescence spectroscopy, the thioflavin T (ThT) binding assay, Congo red staining, and fluorescence microscopy. Its effects on hIAPP-aggregate-mediated β cell death were studied by a formazan-dye reduction cell viability assay and by assessment of apoptosis.

Results

The interaction of NF(N-Me)GA(N-Me)IL with hIAPP and its interference with the β sheet and amyloid-fibril formation process were first studied by a previously established far-UV CD/EM experimental system [13, 33]. For the CD experiments, we used a 5 μM hIAPP solution (10 mM phosphate buffer [pH 7.4], 1% HFIP), which we have previously found to correspond to a kinetically soluble but supersaturated hIAPP solution [34]. The presence of small amounts (1%–4%) of HFIP in hIAPP solutions has been found by us and others to synchronize and/or enhance hIAPP fibrillogenesis processes [12–14]. Of note, to ensure that the observed effects on hIAPP conformation were due to hIAPP-peptide interaction, all solutions tested, including hIAPP alone, the mixtures of hIAPP with the peptides, and the peptides alone, contained the same final HFIP concentration of 1%. hIAPP alone was initially soluble and in a predominantly unordered state and aggregated after a lag time of 7 days into β sheets (Figure 1B) [13, 35, 36]. At this time point, insoluble aggregates appeared, and EM after centrifugation showed that they consisted mainly of amyloid fibrils (Figure 1D). In the presence of NF(N-Me)GA(N-Me)IL (at a 10-fold molar excess), however, the solution was clear, and no aggregation into β

sheets was observed for up to 14 days (Figure 1C). No changes were observed in the UV spectrum during the 14 days, indicating that hIAPP was in a soluble state. EM examination at various time points indicated the absence of amyloid fibrils or other ordered aggregates (Figure 1E).

The spectrum of the hIAPP/NF(N-Me)GA(N-Me)IL mixture (1:10 ratio) at time 0 after the begin of incubation strongly differed from the sum of the spectra of each component alone (at time 0), suggesting that NF(N-Me)GA(N-Me)IL interacted with hIAPP [22]. The spectrum of the mixture of hIAPP with NF(N-Me)GA(N-Me)IL had a strong minimum at 225–228 nm, a weak minimum at 202–205 nm, and a weak maximum at 210 nm (Figure 1C). Notably, this spectrum showed significant fluctuations during the study. Therefore, the $[\theta]_{225-228}$ value (turn/β sheet) became less while the $[\theta]_{202-205}$ value (random coil) increased by a similar amount and vice versa (Figure 1C). CD spectra of NF(N-Me)GA(N-Me)IL alone (50 μM) showed no time-dependent conformational changes, indicating that the fluctuations might be due to the interaction of NF(N-Me)GA(N-Me)IL with hIAPP. Of note, even when hIAPP was mixed with NF(N-Me)GA(N-Me)IL at an 1:1 or 1:0.1 ratio, in which low or no contribution of the CD spectrum of NF(N-Me)GA(N-Me)IL to the CD spectrum of the mixture was observed, the shapes of the spectra were very similar to the spectrum of the 1:10 mixture (data not shown). However, NF(N-Me)GA(N-Me)IL was not able to significantly inhibit β sheet formation and to delay hIAPP insolubilization at hIAPP/NF(N-Me)GA(N-Me)IL molar ratios of 1:1 and 1:0.1.

We next examined the effect of NFGAIL on hIAPP aggregation into β sheets and amyloid fibrils by CD and EM [20, 29]. Although NFGAIL is an amyloidogenic peptide per se, it has a high kinetic solubility (in the milimolar range) as compared to IAPP (in the nanomolar range) [29]. Therefore, it was expected that NFGAIL would remain soluble during the time course of the CD study. In Figure 2A, CD spectra of an hIAPP solution (5 μM) before and after addition of NFGAIL (50 μM) for up to 14 days are shown. At 14 days, insoluble amyloid fibrils precipitated out of solution (Figure 2B). RP-HPLC analysis of the precipitate after resolubilization in DMSO showed that the aggregates consisted exclusively of hIAPP (data not shown). The conformation and solubility of NFGAIL (50 μM) were also followed over time, and no changes or precipitation were observed for 14 days. Although the CD studies indicated that NFGAIL could not inhibit hIAPP amyloidogenesis, the fluctuations of the spectrum of the mixture and the marked difference between the spectrum of the mixture at time 0 from the sum of the spectra of each peptide (at time 0) indicated that NFGAIL interacted with hIAPP [20]. The effect of the rat IAPP (rIAPP) sequence rIAPP(22–27) or NLGPVL on hIAPP was next examined by CD/EM (Figures 2C and 2D). This sequence, although partially homologous to hIAPP(22–27) or NFGAIL, has no amyloidogenic properties [29, 37, 38]. When hIAPP was incubated with NLGPVL (50 μM), insoluble hIAPP amyloid fibrils—as confirmed by EM and RP-HPLC analysis of the resolubilized aggregates—precipitated at 5 days (Figures 2C and 2D). We also tested the effect of the scrambled N-methylated sequence (N-Me)IAF(N-Me)GNL (50 μM) on the conformational transition of hIAPP (5 μM) into β sheets and amyloid formation by CD and EM. No inhibition of the aggregation into β sheets and amyloid formation was observed (data not shown).

The thioflavin-T assay was next used to obtain a quantitative estimation of the effect of NF(N-Me)GA(N-Me)IL and the control peptides on hIAPP fibrillogenesis (Figures 3A and 3B). Amyloid fibrils of polypeptides and proteins, including hIAPP, bind the dye ThT, and the increase in ThT fluorescence emission is broadly used as a specific and quantitative assay for fibril formation [39, 40]. In contrast to the conditions used for the CD studies, the ThT assay was performed in the absence of HFIP (6.25 μM hIAPP in aqueous Tris buffer [pH 7.4]) because according to studies by us and others, HFIP, even at 1%–2%, results in a strong acceleration of hIAPP fibrillization [14, 41]. However, a ThT system describing the complete pathway, including both pre- and postnucleation, is required to investigate the effect of potential inhibitors on fibrillogenesis. The profile of hIAPP-fibril formation obtained was consistent with nucleation-dependent fibrillogenesis and showed a lag time of about 50 hr (Figure 3A). Thereafter, a steep increase in ThT fluorescence was observed that correlated with an increase in the amount of amyloid fibrils, which was confirmed by EM. Fluorescence increase was followed by a plateau, which indicated the end of the fibrillization process. In the presence of NF(N-Me)GA(N-Me)IL (10-fold excess), however, the lag time was longer, and the ThT fluorescence was markedly less than in the hIAPP solution after 14 days (Figure 3A). NF(N-Me)GA(N-Me)IL also inhibited hIAPP fibrillogenesis significantly when it was applied at a 10-fold lower concentration (625 nM) than hIAPP (Figure 3A). Inhibition was stronger when NF(N-Me)GA(N-Me)IL was applied at a 10-fold excess than at a 10-fold lower concentration than hIAPP (Figure 3A). The kinetic profiles of ThT assays suggested that NF(N-Me)GA(N-Me)IL caused both a significant elongation of the lag time and a reduction of the amount of fibrils formed. However, NF(N-Me)GA(N-Me)IL (up to a 10-fold excess) did not completely stop the hIAPP amyloidogenesis process. In other ThT experimental sets, we addressed the question of whether NF(N-Me)GA(N-Me)IL was able to stop already seeded hIAPP amyloid-fibril formation processes. These experiments were performed in buffers containing 1% or 2% HFIP and indicated that NF(N-Me)GA(N-Me)IL (10-fold excess) delayed but did not stop fibrillogenesis (data not shown). Strong effects of the applied buffers and HFIP contents on the inhibitory effect on fibrillogenesis were also observed in these studies. No inhibition of hIAPP fibrillogenesis was observed by the control peptides NFGAIL, (N-Me)IAF(N-Me)GNL, and the N-methylated peptide AA(N-Me)GA(N-Me)VV that was derived from human prion protein PrP(117–122) and is homologous to NF(N-Me)GA(N-Me)IL (Figure 3B).

A detailed EM study of solutions of ThT assays was performed next (Figures 4A–4F). In Figures 4A–4D, species present in the ThT solution of hIAPP (Figure 3A) and the mixtures of hIAPP/NF(N-Me)GA(N-Me)IL (1:10) at 14 days (endpoint of fibrillization) are shown. The hIAPP solutions consisted mainly of mature fibrils (Fig-

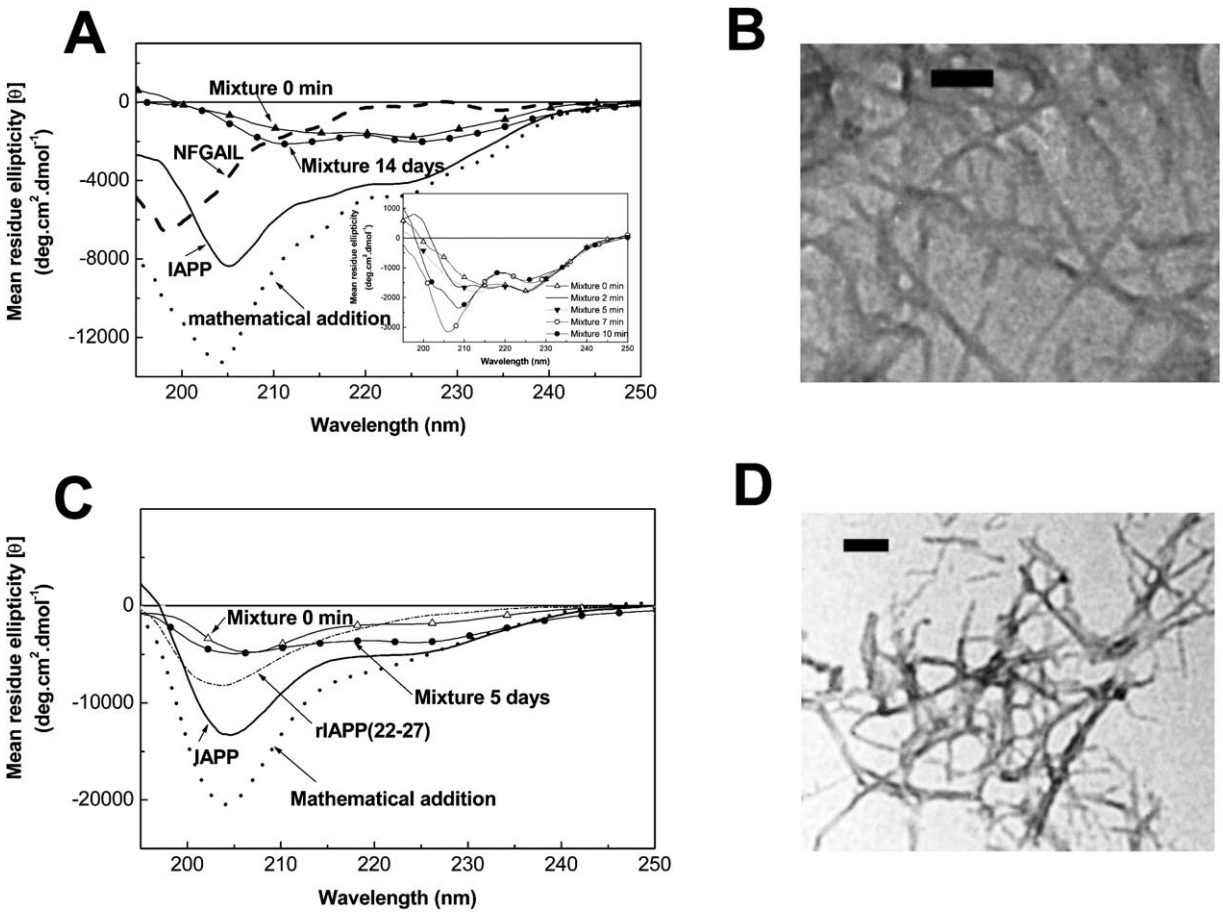

Figure 2. Interactions of hIAPP(22–27) or NFGAIL and rIAPP(22–27) or NLGPVL with hIAPP and Effect on hIAPP Amyloid-Fibril Formation as Assessed by CD and EM

(A) CD spectra of the mixture of hIAPP (5 μM) with NFGAIL (50 μM) at time 0 min after the begin of the incubation and at 14 days are shown. At this time point, insoluble hIAPP aggregates appeared. For comparison, the spectrum of hIAPP alone (at 0 min), of NFGAIL alone, and of the mathematical addition of the CD spectra of hIAPP alone (at 0 min) and of NFGAIL alone (at 0 min) are also shown. In the inset, representative spectra of the mixture recorded between 0 and 10 min after the begin of the incubation are shown.

(B) Representative electron micrograph of the hIAPP with NFGAIL solution of the CD experiment of (A) after incubation for 14 days and peptide insolubilization. The bar represents 100 nm.

(C) CD spectra of the mixture of hIAPP (5 μM) with rIAPP(22–27) (NLGPVL) (50 μM) at the time point 0 min and 5 days later are shown. At this time point, insoluble hIAPP aggregates appeared. The spectrum of hIAPP alone (at 0 min), of NLGPVL alone (at 0 min), and of the mathematical addition of the hIAPP and NLGPVL spectra (at 0 min) are shown.

(D) Representative electron micrograph of the hIAPP with NLGPVL mixture of the CD experiment of (A) after incubation for 5 days and peptide insolubilization. The bar represents 100 nm.

ure 4A). By contrast, the hIAPP/NF(N-Me)GA(N-Me)IL (1:10) mixture (Figure 3A) consisted mainly of amorphous aggregates, ordered spherical species, short curly protofibril-like species, and mature fibrils (Figures 4B–4D). Ordered spherical and protofibril-like species were also main species in prenucleated mixtures of hIAPP/NF(N-Me)GA(N-Me)IL (1:10) (i.e., incubations in Tris buffer containing 1% HFIP) (Figures 4E and 4F). Figure 4E shows that short curly protofibrils and spherical aggregates were the main species present at 8 hr after the begin of incubation, whereas Figure 4F shows that at 24 hr, mainly spherical species and mature fibrils were present. A solution of hIAPP alone under these conditions and at 24 hr consisted mainly of mature fibrils. These results indicated that the presence of NF(N-Me)GA(N-Me)IL might have resulted in stabilization of pre- and/or protofibrillar hIAPP species. Of note, the 14-day-old ThT-assay mixtures of hIAPP with NFGAIL and (N-Me)IAF(N-Me)GNL (also at 1:10) contained mainly mature hIAPP fibrils.

We next tested if NF(N-Me)GA(N-Me)IL could affect the cytotoxic effect of hIAPP aggregates on the pancreatic insulinoma cell line RIN5fm by using two-cell viability assays. The first assay was the 3-[4,5-dimethylthiazol-2-yl]-2,5-diphenyltetrazolium bromide (MTT) reduction assay that gives information about cellular redox ability (Figure 5A). The latter one is a specific, early indicator of cell viability [42–44]. Because amyloid-mediated cytotoxicity is associated with reduced cellular redox potential, this assay has found broad application for studying the toxicity of amyloidogenic peptides [7, 15, 22, 29, 42–45]. Serial dilutions of a solution of

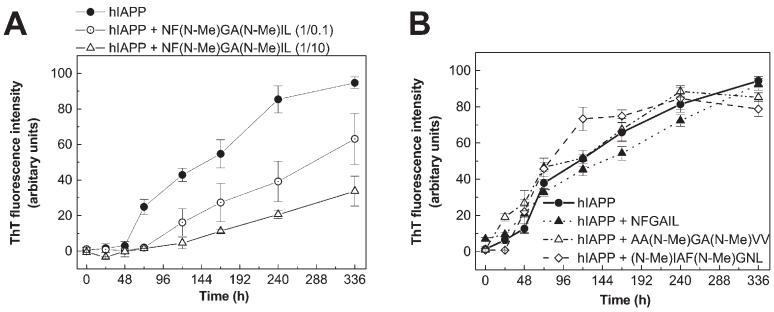

Figure 3. Effects of NF(N-Me)GA(N-Me)IL and Various Control Peptide Sequences on hIAPP Fibrillogenesis as Assessed by the ThT Binding Assay

(A) ThT fluorescence versus time of hIAPP (6.25 μM) solutions or solutions of hIAPP (6.25 μM) with NF(N-Me)GA(N-Me)IL (62.5 μM and 625 nM).

(B) ThT fluorescence versus time of hIAPP (6.25 μM) solutions or solutions of hIAPP (6.25 μM) with the control peptides NFGAIL, AA(N-Me)GA(N-Me)VV, and (N-Me)IAF(N-Me)GNL (625 nM). Similar results to the above were obtained when the control peptides were applied at 10-fold excess (62.5 μM) as compared to hIAPP. Data are the mean ± SEM of three to six independent experiments.

seedless hIAPP (5 μM) with or without NF(N-Me)GA(N-Me)IL (at 50 μM or 500 nM) were applied for 20 hr onto the cells. After addition of MTT, cellular MTT reduction was assessed [29]. The hIAPP/NF(N-Me)GA(N-Me)IL mixtures both at a 1:10 and a 1:0.1 molar ratio were significantly less cytotoxic than hIAPP alone, suggesting that NF(N-Me)GA(N-Me)IL is an effective inhibitor of hIAPP toxicity (Figure 5A). Parts of the solutions that were added to the cells were also examined by EM. Amorphous aggregates and spherical hIAPP species were present, whereas no mature amyloid fibrils were detected (data not shown). It should be noted that the effect of NF(N-Me)GA(N-Me)IL on hIAPP cytotoxicity strongly depended on the aggregation and nucleation

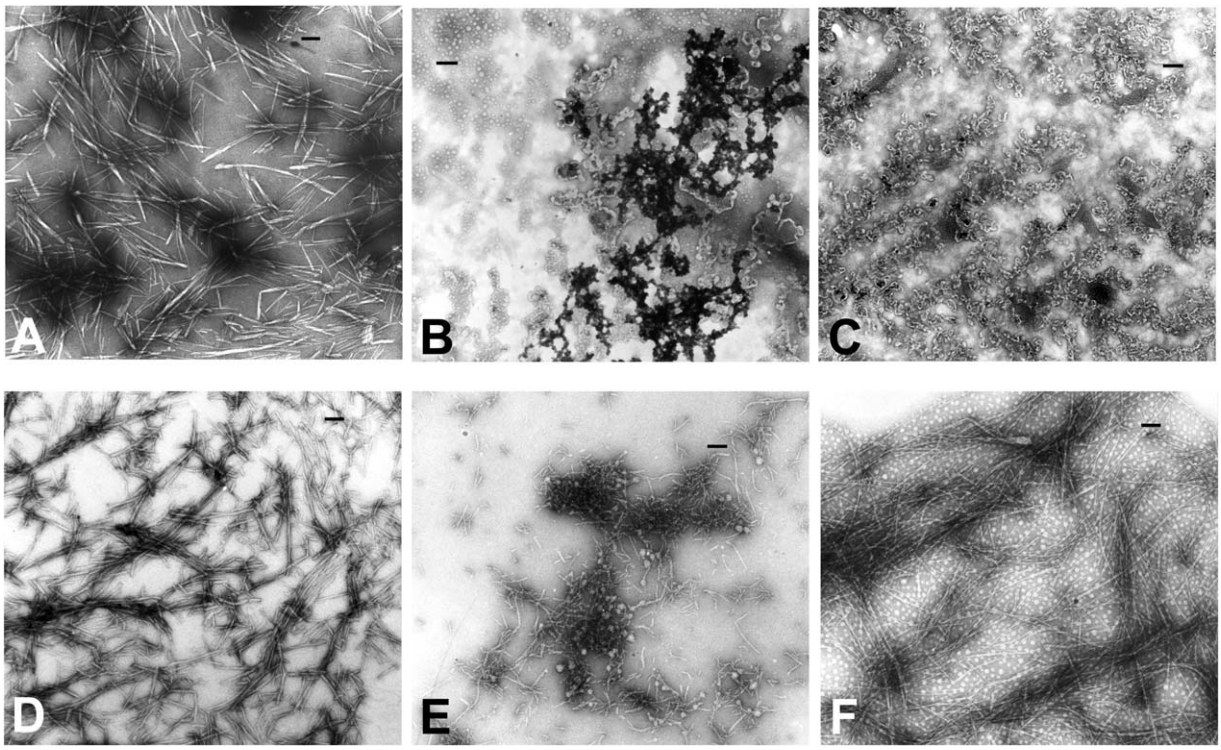

Figure 4. Inhibition of hIAPP Fibrillogenesis by NF(N-Me)GA(N-Me)IL as Assessed by EM

(A) A representative electron micrographs of an hIAPP-alone incubation (6.25 μM in Tris buffer [pH 7.4]) (incubation from Figure 3A) at 14 days that consisted mainly of mature fibrils.

(B–D) Representative electron micrographs of an hIAPP/NF(N-Me)GA(N-Me)IL (1:10) (6.25 μM hIAPP in Tris buffer [pH 7.4]) mixture at 14 days (incubation from Figure 3A) that consisted of amorphous aggregates (B), ordered spherical species (B), protofibril-like species (C), and mature fibrils (D) are shown.

(E and F) Representative electron micrographs of an hIAPP/NF(N-Me)GA(N-Me)IL incubation (1:10) (6.25 μM hIAPP, in Tris buffer [pH 7.4] with 1% HFIP) at 8 hr (E) and 24 hr (F). At 8 hr, the solution consisted mainly of short protofibril-like species and ordered spherical aggregates (E). At 24 hr, mature fibrils and round spherical aggregates were the main species present (F).

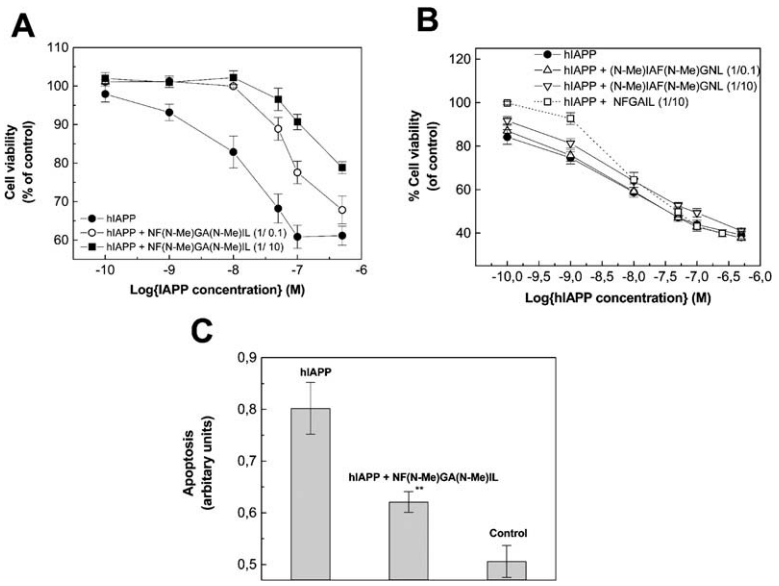

Figure 5. Effects of NF(N-Me)GA(N-Me)IL and Various Control Peptide Sequences on hIAPP Cytotoxicity towards RIN 5fm Cells as Assessed by the MTT Reduction Assay and an Apoptosis Assay

(A and B) Cell viability in the presence of various concentrations of hIAPP alone versus mixtures of hIAPP with NF(N-Me)GA(N-Me)IL (1:10 and 1:0.1) (A) or the control peptide sequences NFGAIL (1:10) and (N-Me)IAF (N-Me)GNL (1:10 and 1:0.1) as indicated. Cell viability was assessed after 20 hr incubation of the above solutions with the cells via the MTT reduction assay. Data are percentages of control values and are the mean ± SEM of at least four independent experiments with each experiment performed in multiple replicates (n = 4) except for the data of the NFGAIL/hIAPP mixture, which are from one representative experiment performed in triplicate.

(C) Apoptotic effect of hIAPP alone (500 nM) versus a mixture of hIAPP (500 nM) with NF(N-Me)GA(N-Me)IL (50 nM) on RIN 5fm cells. Apoptosis was assessed after 20 hr incubation of the above solutions with the cells by ELISA quantification of cytosolic histone-associated nucleosomes. The data shown are from three independent experiments with each experiment performed in multiple replicates (n = 4). The inhibitory effect of NF(N-Me)GA(N-Me)IL on hIAPP cytotoxicity was statistically significant ($p < 0.01$ by ANOVA) (indicated by double asterisks). The difference between the effect of vehicle alone versus hIAPP was also statistically significant ($p < 0.001$).

state of hIAPP at the begin of incubation, and no significant inhibitory effects were found in prenucleated solutions. No inhibition of cytotoxicity was found in hIAPP mixtures with AA(N-Me)GA(N-Me)VV, NFGAIL, and (N-Me)IAF(N-Me)GNL (Figure 5B).

It has been shown that β cell death caused by hIAPP aggregates is mainly due to apoptosis [7, 8, 15, 46, 47]. We therefore studied the effect of NF(N-Me)GA(N-Me)IL on hIAPP-mediated apoptosis of RIN5fm cells (Figure 5C). We studied the effect of NF(N-Me)GA(N-Me)IL at a molar ratio of hIAPP/NF(N-Me)GA(N-Me)IL of 1:0.1 because according to the MTT assay, this ratio was sufficient for a marked inhibition of hIAPP cytotoxicity. Quantification of apoptosis was performed via quantification of cytoplasmatic histone-associated nucleosomes that are early indicators of apoptotic cell death [48, 49]. hIAPP (500 nM) with or without NF(N-Me)GA(N-Me)IL (50 nM) was incubated for 20 hr with the cells and after cell lysis, histone-associated nucleosomes were quantified by an ELISA [47, 49]. As shown in Figure 5C, NF(N-Me)GA(N-Me)IL markedly inhibited hIAPP-aggregate-mediated apoptotic cell death.

Fluorescence spectroscopy was applied by using synthetic, N^{α}-terminal-fluorescein-labeled hIAPP (Fluos-hIAPP) to further characterize the interaction of NF(N-Me)GA(N-Me)IL with hIAPP. In preliminary studies, we found that N^{α}-terminal labeling of hIAPP with fluorescein did not significantly affect the amyloidogenic properties of hIAPP (L.-M.Y., M.T.-N., A. Velkova, A. Kazantzis, and A.K., unpublished data). We also titrated Fluos-hIAPP (1 nM) with hIAPP (10 pM–1 μM) and determined an apparent K_d of 10 nM for the Fluos-hIAPP-hIAPP complex (L.-M.Y., M.T.-N., A. Velkova, A. Kazantzis, and A.K., unpublished data). To date, there have been no reports about the affinity of the hIAPP-hIAPP interaction. Biophysical studies have suggested, however, that it might be in the nanomolar range, which would be in good agreement with the value determined by our fluorescence assay [8, 13, 14]. A directly proportional concentration dependence was found for the fluorescence signal of Fluos-hIAPP alone between 1 and 4 nM. The above data suggested that 1 nM Fluos-hIAPP was either monomeric or at a stable monomeric/oligomeric state at this low concentration range. Addition of NF(N-Me)GA(N-Me)IL at a 1000-fold molar excess (1 μM) to the Fluos-hIAPP solution (1 nM) resulted in a 100% enhancement of the fluorescence intensity of Fluos-hIAPP (Figure 6A). This result suggested that NF(N-Me)GA(N-Me)IL binds monomeric and/or soluble oligomeric hIAPP, and binding results in a change in the environment of the fluorescein label. Titration of 1 nM Fluos-hIAPP with NF(N-Me)GA(N-Me)IL (10 pM–10 μM) resulted in a sigmoidal curve and an apparent K_d of 129 nM (± 59) (mean ± SEM of three independent binding curves) for the hIAPP-NF(N-Me)GA(N-Me)IL complex (Figure 6B). Of note, no changes in fluorescence of Fluos-hIAPP were found when it was mixed with a 1000-fold molar excess of NFGAIL, (N-Me)IAF(N-Me)GNL, and AA(N-Me)GA(N-Me)VV, suggesting a high specificity of the observed hIAPP-NF(N-Me)GA(N-Me)IL interaction.

We next asked if NF(N-Me)GA(N-Me)IL would also be able to bind and, thus, stain in vivo-formed, insoluble human pancreatic-amyloid deposits. A solution of N-terminal-fluorescein-labeled NF(N-Me)GA(N-Me)IL peptide was applied to a human pancreatic tissue section with an amyloid-containing islet. A consecutive tissue section was stained with Congo red, which is an amyloid-specific dye [1, 50, 51]. Fluorescence microscopy showed that, in fact, the fluorescently labeled peptide

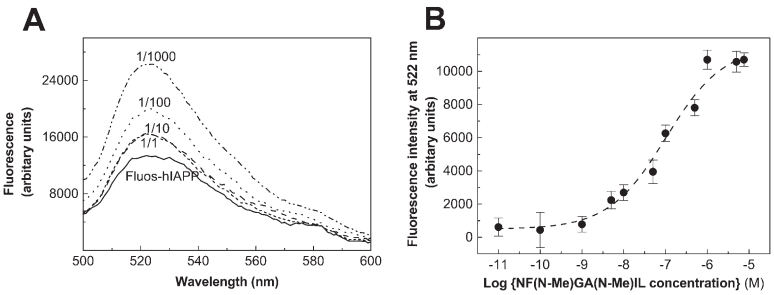

Figure 6. Interaction of NF(N-Me)GA(N-Me)IL with hIAPP as Studied by Fluorescence Spectroscopy

(A) Fluorescence spectra of Fluos-hIAPP (1 nM) alone and after addition of NF(N-Me)GA(N-Me)IL at various concentrations as indicated.

(B) Binding curve (dashed lines) obtained upon titration of Fluos-hIAPP (1 nM) with NF(N-Me)GA(N-Me)IL. The affinity of the interaction was estimated to be 129 nM. Data shown are the mean ± SEM from three independent binding curves (the fluorescence of Fluos-hIAPP alone was subtracted).

(Figure 7A, green fluorescence) binds in vivo-formed amyloid deposits (Figure 7B, red fluorescence). The fluorescently labeled peptide did not bind to nonamyloid-containing pancreatic tissue (Figures 7A and 7B). Other synthetic hIAPP fragments, including hIAPP(1–13) or NFGAIL, did not bind (hIAPP[1–13]) or bound nonspecifically to pancreatic tissue (NFGAIL) (not shown). In addition, no binding of fluorescently labeled NF(N-Me)GA(N-Me)IL on secondary amyloidosis (AA)-derived amyloid deposits of canine glomeruli was found (Figures 7C and 7D). These latter amyloid deposits derive from serum amyloid A (SAA). Although more studies will be necessary to demonstrate the specificity of the staining of human pancreatic amyloid by fluorescently labeled NF(N-Me)GA(N-Me)IL as compared to other types of amyloid deposits, this latter result offers a first indication that this might be the case.

Discussion

Based on a structure-based, selective N-methylation-design approach, we have recently converted short, amyloidogenic hIAPP self-recognition sequences into soluble, nonamyloidogenic and noncytotoxic ones [22]. Based on the hypothesis that these sequences may contain an important hIAPP self-recognition element, they were also expected to be able to interact with hIAPP and interfere with its amyloid-forming pathway [8, 52, 53]. One of the designed sequences is NF(N-Me)GA(N-Me)IL that has been derived via rational N-methylation of the hIAPP amyloid-core hexapeptide hIAPP (22–27) or NFGAIL [29–31, 54]. Here, we studied the ability of NF(N-Me)GA(N-Me)IL to interact with hIAPP, both in its soluble and in its pancreatic-amyloid form, to interfere with the fibrillogenesis process of hIAPP and to inhibit its amyloid-forming potential and related toxicity toward β cells.

CD studies and EM suggested that NF(N-Me)GA(N-Me)IL was in fact able to interact with hIAPP and to inhibit its transition into aggregated β sheets and insoluble amyloid fibrils when applied at a 10-fold molar excess [8, 11, 13, 36]. The CD studies also indicated that NF(N-Me)GA(N-Me)IL was able to interact with hIAPP when it was also at a 10-fold-lower concentration than hIAPP, whereas no inhibition of hIAPP fibrillogenesis was observed under these conditions. Because CD refers to overall conformation and because both peptides may change their conformation upon interaction, it was not possible to determine by this method the conformation that hIAPP adopted after interaction with NF

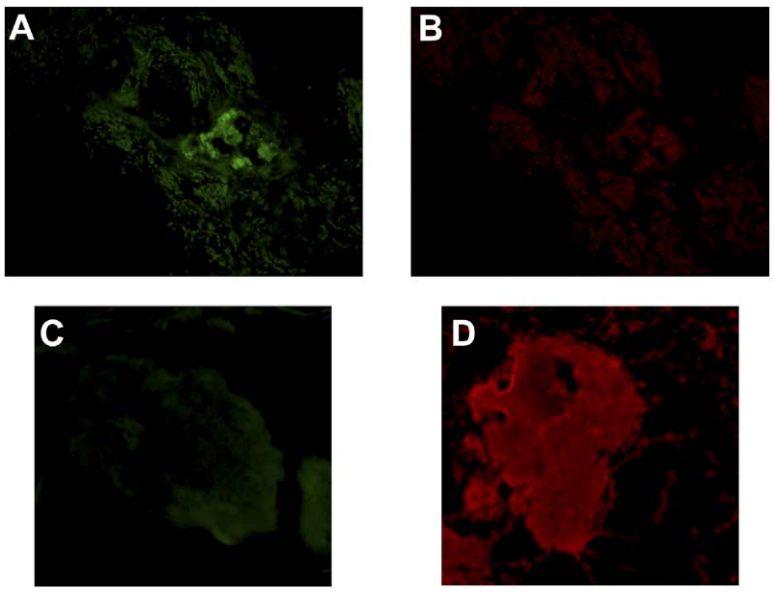

Figure 7. Interaction of Fluorescein-Labeled NF(N-Me)GA(N-Me)IL with IAPP or AA Amyloid-Containing Tissues as Studied by Fluorescence Microscopy

(A and B) Fluorescence microscopy of consecutive human pancreatic tissues containing amyloid deposits after staining with fluorescently labeled NF(N-Me)GA(N-Me)IL (green) (A) and Congo red (red) (B) (magnification 200×).

(C and D) Fluorescence microscopy of consecutive canine renal tissues with AA amyloid after staining with fluorescently labeled NF(N-Me)GA(N-Me)IL (C) and Congo red (D) (magnification 40×).

(N-Me)GA(N-Me)IL. However, the very low kinetic solubility of hIAPP (low micromolar to nanomolar range) precluded the use of other biophysical methods, including NMR or FT-IR. The CD spectra of the various hIAPP/NF(N-Me)GA(N-Me)IL mixtures were characterized by a reduced magnitude, in particular in the random coil area, as compared to the spectrum of hIAPP alone, whereas their shape was clearly indicative of the presence of significant amounts of ordered structure, i.e., β turn- and/or β strand-containing conformeric states [22, 25–27, 35, 55, 56]. The observed conformational ordering in the hIAPP/NF(N-Me)GA(N-Me)IL mixtures might reflect formation of ordered hIAPP-NF(N-Me)GA (N-Me)IL complexes and/or an NF(N-Me)GA(N-Me)IL-induced stabilization of soluble hIAPP oligomers [14, 41]. According to the design strategy, interaction of NF(N-Me)GA(N-Me)IL with soluble hIAPP species might have resulted in formation of ordered heterodimers and/or heteromultimers [22]. In fact, detailed EM studies suggested that ordered oligomeric assemblies including prefibrillar spherical species and protofibril-like species formed.

The ThT/EM studies showed that NF(N-Me)GA(N-Me) IL, at a 10-fold molar excess, was able to markedly delay hIAPP fibrillogenesis and to strongly reduce the amount of mature fibrils. Both findings were in good agreement with the results of the CD studies. The ThT assay also showed that NF(N-Me)GA(N-Me)IL was able, even at a 10-fold-less concentration than hIAPP, to inhibit fibrillogenesis, albeit less effectively than at a 10-fold-higher concentration. However, the results of the ThT/EM assays also showed that NF(N-Me)GA(N-Me)IL was not able to completely block hIAPP fibrillogenesis. At first sight, these latter results appear to be contradictory to the results of the CD/EM studies, which indicated an absence of fibrillar or other ordered aggregates in the hIAPP/NF(N-Me)GA(N-Me)IL (1:10) mixtures. Potential reasons for the lack of detection of soluble protofibrillar species include their possible adherence on the windows of the CD cuvette and the possibility that the examined EM samples did not contain all aggregate species. This could be due to the fact that the CD solutions have not been agitated before removing samples for EM because the smallest disturbance of such supersaturated solutions may result in aggregation [34]. On the other hand, it is also likely that no soluble ordered species or protofibrils were formed in the CD solutions, contrary to what was observed in the ThT solutions, because of the different experimental conditions used in the two assays: the CD/EM assay was performed in aqueous phosphate buffer containing 1% HFIP with 5 μM hIAPP, whereas for the ThT/EM assay, a non-HFIP-containing Tris buffer system with 6.25 μM hIAPP was applied. The 1% HFIP conditions were well suited for obtaining a kinetically stable but supersaturated hIAPP solution in the CD cuvette. However, when we applied exactly the same experimental conditions as the ones used for the CD experiments to perform incubations in eppendorf tubes and examined the incubations with the ThT assay conditions, strongly prenucleated systems with no lag times were obtained. These results were not unexpected as it is well known how strongly small differences between experimental systems may affect the kinetics and thermodynamics of protein oligomerization and fibrillogenesis [34, 57]. The above observations point out the limitations of the use of a CD assay alone or in combination with EM and underline the importance of the use of a combination of different assay systems and experimental conditions to quantify the inhibitory potentials of compounds designed to intervene with multistep processes such as the protein and polypeptide fibrillization processes [13, 57].

Taken together, the CD, EM, and ThT assay results suggested that NF(N-Me)GA(N-Me)IL strongly interfered with the β sheet formation and fibrillogenesis pathway of hIAPP and inhibited formation of mature fibrils. In addition, these results indicated that the observed inhibitory effect of NF(N-Me)GA(N-Me)IL on hIAPP fibrillogenesis might most likely be due to its interaction with monomeric or oligomeric IAPP species. Interaction appears to cause a delay of nucleus formation and, thus, of the beginning of the fibrillogenesis process, a stabilization of pre- or protofibrillar species, and a reduction of the amount of mature fibrillar IAPP aggregates. Of note, no inhibitory effects on hIAPP fibrillogenesis with CD, EM, and ThT assays were found for a number of control hexapeptides including NFGAIL, rIAPP(22–27), AA(N-Me)GA(N-Me)VV, and (N-Me)IAF (N-Me)GNL.

Direct evidence for the ability of NF(N-Me)GA(N-Me) IL to bind soluble monomeric and/or oligomeric hIAPP species was obtained by fluorescence titration studies of Fluos-hIAPP with NF(N-Me)GA(N-Me)IL. The changes in fluorescence of fluorescently labeled proteins or polypeptides are highly sensitive indicators of changes in their environment such as changes that might be caused by ligand binding or self-association [58–60]. An important advantage in applying fluorescence-based methods for the assessment of ligand binding to a polypeptide with high aggregation propensity, such as hIAPP, is their high sensitivity [58]. The latter one allows for very low concentrations of proteins/polypeptides, i.e., concentrations where the polypeptide might be in a nonaggregated state, to be used. In fact, our studies indicated that Fluos-hIAPP at 1 nM was most likely at a stable monomeric and/or early oligomeric state (or states). Binding of NF(N-Me)GA(N-Me)IL to Fluos-hIAPP caused a strong change in the environment of the N-terminal-fluorescein label, suggesting that binding is most likely associated with a strong change of conformation and/or assembly state (or states) of monomeric or oligomeric hIAPP. An apparent dissociation constant of 129 nM was derived from the binding isotherm and suggested a high affinity for the hIAPP-NF(N-Me)GA(N-Me)IL interaction. Importantly, NFGAIL, (N-Me)IAF(N-Me)GNL, and AA(N-Me)GA(N-Me) VV did not cause any changes in the fluorescence emission of Fluos-hIAPP, even at 1000-fold-higher concentrations than Fluos-hIAPP. These latter results indicated that these peptides either might have not bound Fluos-hIAPP species present at 1 nM or that they might have bound, but binding did not induce changes in the enviroment of the N-terminal-fluorescein label. Regarding the NFGAIL-hIAPP interaction, both interpretations would not be contradictory to the CD results, which indicated that NFGAIL interacted with hIAPP. One reason for this is that the CD studies were performed at a

5000-fold-higher hIAPP concentration than the fluorescence measurements. Moreover, these findings suggested that NFGAIL might bind hIAPP either in a different mode or much weaker than NF(N-Me)GA(N-Me)IL, which might account for the observed inability of NFGAIL to inhibit hIAPP fibrillogenesis and cytotoxicity.

Ten years ago, insoluble mature amyloid fibrils were suggested to cause the cytotoxic effect of hIAPP [7]. However, in the past few years, evidence has been accumulated that suggests that soluble, not yet identified, hIAPP oligomers might be the main mediators of hIAPP-amyloid-associated cell toxicity [8–11]. Soluble aggregates have been suggested to permeabilize cell membranes via a channel- or pore-like mechanism or simply by causing small membrane defects [9, 10, 12, 15, 61]. An important implication of these findings for the design of inhibitors of hIAPP cytotoxicity is that—depending on the mechanism of its action—a compound that inhibits hIAPP-amyloid formation may not necessarily inhibit cytotoxicity and vice versa [62]. The synthetic peptide hIAPP(24–29) or GAILSST, for example, has been reported to reduce hIAPP amyloid formation but was unable to affect its cytotoxicity, and organic compounds that inhibited hIAPP cytotoxicity or membrane activity did not inhibit amyloid-fibril formation [15, 16, 18–20, 63].

We tested the effect of NF(N-Me)GA(N-Me)IL on hIAPP β cell toxicity by using two different cytotoxicity assays. First, the MTT reduction assay was applied [43, 44]. NF(N-Me)GA(N-Me)IL was found to significantly reduce hIAPP cytotoxicity even at a molar ratio of NF(N-Me)GA(N-Me)IL to hIAPP of 0.1 to 1. By contrast, no inhibitory effect was found for the control peptides NFGAIL, AA(N-Me)GA(N-Me)VV, and the scrambled N-methylated sequence (N-Me)IAF(N-Me)GNL. We also studied the effect of NF(N-Me)GA(N-Me)IL on hIAPP-mediated β cell apoptosis [7, 15, 46, 47]. Assessment of apoptotic death is not only an additional method to the MTT reduction for determining cell viability but also represents a highly sensitive technique to investigate the mechanism of cell death and/or its inhibition [46–49]. The results were consistent with the results of the MTT assay and showed that NF(N-Me)GA(N-Me)IL at a 0.1 molar ratio to hIAPP significantly reduced hIAPP apoptosis of β cells. For comparison, hIAPP(20–25) or SNNFGA, which is the only other reported peptide inhibitor of hIAPP cytotoxicity, reduces hIAPP cytotoxicity at a 20-fold molar excess as compared to hIAPP [20].

The results of our studies also suggested that NF(N-Me)GA(N-Me)IL was unable to completely inhibit hIAPP fibrillogenesis and cytotoxicity. These findings are consistent with the results of the fluorescence-based hIAPP binding assay. Thus, it appears possible that NF(N-Me)GA(N-Me)IL might interact with monomeric or β sheet edge strands of soluble, β sheet hIAPP oligomers, most likely similarly to a NFGAIL-containing β strand of full-length hIAPP [22]. Alignment of a strand of the N-methylated peptide on a growing β sheet oligomer would, possibly, prohibit or delay further sheet extension because of interruption of the H-bonding potential of the edge hIAPP strand [22]. On the other hand, the highly cooperative nature of the hIAPP self-assembly and fibrillogenesis processes and the high affinity of the Fluos-hIAPP-hIAPP interaction, which according to our fluorescence binding assay, was estimated to be about 13-fold-stronger than the affinity of the Fluos-hIAPP-NF(N-Me)GA(N-Me)IL interaction, might account for the lack of NF(N-Me)GA(N-Me)IL to completely abolish fibrillogenesis, to stop already-nucleated amyloidogenesis processes, and to completely inhibit their cytotoxic effects [14, 41].

More detailed studies will be necessary to fully understand the mechanism of inhibition of hIAPP fibrillogenesis and cytotoxicity by NF(N-Me)GA(N-Me)IL. Taken together, however, the results of our studies were consistent with each other and suggested that NF(N-Me)GA(N-Me)IL is able to delay and reduce the extent of hIAPP fibrillogenesis and to reduce the cytotoxic effect of hIAPP aggregates. The inhibitory effects were strongest when the inhibitor was applied at a 10-fold molar excess, whereas significant effects were observed even at a 10-fold-lower inhibitor concentration as compared to hIAPP. According to our EM, ThT, and CD studies, the observed reduction of cytotoxicity of IAPP in the presence of NF(N-Me)GA(N-Me)IL was associated with the formation or stabilization of pre- or nonfibrillar spherical oligomeric assemblies. These latter assemblies and/or their dissociation products appear to cause less damage to the cells than the assemblies of the IAPP-alone solutions and consist of either IAPP-IAPP or IAPP-NF(N-Me)GA(N-Me)IL complexes. The detailed biophysical characterization of these assemblies and their comparison with the potentially cytotoxic prefibrillar IAPP species reported before will allow for understanding IAPP β cell toxicity [8–11].

Our results also suggested that the presence of the N-methyl rests at Gly24 and Ile26 in the hIAPP self-recognition sequence NFGAIL is a necessary structural requirement for the high-affinity binding of NF(N-Me)GA(N-Me)IL to hIAPP and its inhibitory effect on hIAPP fibrillogenesis and cell toxicity. NF(N-Me)GA(N-Me)IL is a strongly conformationally constrained hexapeptide [22, 26, 35]. The reduced entropic barrier of NF(N-Me)GA(N-Me)IL toward binding to hIAPP, its specific conformational features, and its nonamyloidogenic character, as compared to the nonconstrained and amyloidogenic sequence NFGAIL, might underlie the high-affinity binding of NF(N-Me)GA(N-Me)IL to hIAPP and its inhibitory potential on both hIAPP fibrillogenesis and cytotoxicity [26].

Finally, fluorescently labeled NF(N-Me)GA(N-Me)IL was found to be able to bind and stain in vivo-formed human pancreatic-amyloid deposits [64]. This is the first report of a partial hIAPP sequence (or an analog thereof) that stains in vivo-formed pancreatic-amyloid deposits. Although labeled hIAPP or several hIAPP partial sequences might possibly also be able to bind or stain pancreatic amyloid, their potential use as noninvasive pancreatic-amyloid diagnostic probes would be strongly limited because of synthetic difficulties, their high aggregation propensities, their low solubilities, and/or their cytotoxic effects [8, 29]. Therefore, the significance of this latter finding might be associated with the improved biophysical properties of NF(N-Me)GA(N-Me)IL, including high solubility, no cytotoxicity, and, possibly, enhanced proteolytic stability and its simpler synthesis as compared to hIAPP and its agregation-prone fragments [22, 26, 65]. Labeled NF(N-Me)GA(N-

Me)IL or its analogs could thus be candidates for potential applications as noninvasive diagnostic probes for type II diabetes [1, 22, 66].

Based on the above results, we conclude that NF(N-Me)GA(N-Me)IL is a potent inhibitor of hIAPP fibrillogenesis and cell death. This hexapeptide is the first reported, designed nanomolar affinity hIAPP ligand and the first N-methylated hIAPP amyloid-core-containing inhibitor of full-length hIAPP fibrillogenesis and cell death. Therefore, the data presented here offer a clear proof of principle of the applicability of the amyloid-core-selective N-methylation strategy to the design of inhibitors of hIAPP amyloidogenesis and cytotoxicity. Because amide bond N-methylation is a well-known strategy to increase in vivo half-life and improve the pharmacological properties of peptidic compounds, NF(N-Me)GA(N-Me)IL may become a lead compound for the development of drugs for the treatment of type II diabetes [26, 65].

Significance

Type II diabetes is a progressive β cell-degenerative disease that affects today about 200 million people worldwide. Cell degeneration and the pathogenesis of this disease are strongly associated with the aggregation of the 37-residue polypeptide hIAPP into pancreatic-amyloid fibrils. The hexapeptide hIAPP(22–27), or NFGAIL, has amyloidogenic and cytotoxic properties and has been suggested to be a hIAPP "amyloid core," i.e., a sequence that participates in hIAPP self-association into β sheets and fibrils. We have recently shown that NFGAIL can be converted into a nonamyloidogenic and noncytotoxic sequence via the rational introduction of N-methyl rests at Gly24 and Ile26. The N-methylated analog NF(N-Me)GA(N-Me)IL has also been found to be able to interact with NFGAIL and to inhibit its fibrillogenesis. Here, we show that NF(N-Me)GA(N-Me)IL is able to bind with nanomolar affinity full length hIAPP and to inhibit its fibrillogenesis. Inhibition is characterized by a delay of the fibrillogenesis onset and a strong reduction of amount of fibrils formed. Most importantly, the N-methylated hexapeptide is shown to significantly reduce hIAPP-aggregate-mediated β cell damage and apoptotic β cell death. Fluorescently labeled NF(N-Me)GA(N-Me)IL is also shown to bind and stain in vivo-deposited human pancreatic amyloid. Studies with control hexapeptides, including NFGAIL, the scrambled sequence (N-Me)IAF(N-Me)GNL, and an N-methylated PrP sequence, suggested a high specificity of the NF(N-Me)GA(N-Me)IL-hIAPP interaction and the related inhibitory effects on hIAPP fibrillogenesis and cytotoxicity. These studies demonstrate that two rationally introduced N-methylations of amide bonds are able to convert a short hIAPP amyloid-core sequence into a high-affinity hIAPP ligand that is also able to inhibit hIAPP fibrillogenesis and cytotoxicity. Because NF(N-Me)GA(N-Me)IL is a highly soluble, nonamyloidogenic, and noncytotoxic hexapeptide, these results suggest that NF(N-Me)GA(N-Me)IL and/or other rationally N-methylated hIAPP amyloid-core sequences may be promising candidates as inhibitors of, or non-invasive amyloid diagnostic probes for, type II diabetes pathogenesis.

Experimental Procedures

Materials

Synthetic human hIAPP was obtained from Calbiochem-Novabiochem (Bad Soden, Germany), dissolved into HFIP (Aldrich, grade 99%+) at 200–500 μM, filtered over 0.2 μm filter (Milllipore), and stored at 4°C [13, 33]. The exact concentration of hIAPP stock solutions was determined by measuring UV absorbance at 274.5 nm [67].

Peptide Synthesis, Purification, and Characterization

Peptides, including the fluorescein-labeled peptides, were synthesized by Fmoc-solid phase synthetic (SPPS) protocols, purified by RP-HPLC, and characterized by fast atom bombardment mass spectroscopy (FAB-MS) as recently described [22, 29]. The fluorescein label was introduced to the N terminus of synthetic, HPLC-purified NF(N-Me)GA(N-Me)IL in a solution of the peptide (10 mg/ml) in 0.1 M $NaHCO_3$ buffer with DMSO (buffer to DMSO ratio was 1:1) with 5(6)-carboxyfluorescein-N-hydroxysuccinimide ester (Roche Diagnostics GmbH, Mannheim, Germany) in a 3-fold molar excess, and the progress of the reaction was followed by RP-HPLC. After accomplishment of the reaction (5 hr), the labeled peptide was purified by RP-HPLC and characterized by MALDI. N^{α}-terminal-fluorescein-labeled hIAPP was prepared via Fmoc-based SPPS, purified by RP-HPLC, and characterized by MALDI (L.-M.Y., M.T.-N., A. Velkova, A. Kazantzis, and A.K., unpublished data).

Electron Microscopy

10–50 μl aliquots of solutions or suspensions were applied on carbon-coated grids, stained with uranyl acetate as described [13], and examined with a Zeiss EM 109 electron microscope operated at 80 kV or with a Philips EM 400 T electron microscope operated at 60 kV.

Aggregation Assays with CD and EM

Incubations of hIAPP alone (5 μM) or mixtures of hIAPP (5 μM) with inhibitor or control peptides were performed in the CD cuvette in 10 mM sodium phosphate buffer (pH 7.4) (CD assay buffer) containing 1% HFIP (final concentration) as described [8, 13]. CD spectra were collected at various time points with a Jasco J-720 or an AVIV 202SF spectropolarimeter. CD spectra were collected between 195 and 250 nm at 0.2 nm intervals, a response time of 8 s, and at 25°C. CD spectra (mean residue ellipticities [θ]) are presented after subtracting the spectra of buffer alone. At indicated time points, fibril formation was examined by EM (see above) of aliquots of the solutions or pellets of suspensions after centrifugation (10 min at 12,000 × g) and resuspension into 10 μl of bidestilled water.

Thioflavin T Binding Assay

Solutions containing hIAPP (6.25 μM) in 10 mM Tris buffer (pH 7.4) (assay buffer), in the absence or presence of inhibitor or control peptide were incubated for 14 days. At the indicated time points, 40 μl aliquots were diluted into 160 μl of a thioflavin T (ThT) solution (5 μM ThT in 0.1 M glycine/NaOH [pH 8.5]) and ThT binding was measured as described [45]. An increase in fluorescence emission at 486 nm (measured in triplicate) after excitation at 450 nm indicated increased hIAPP amyloid formation. For the 1:0.1 hIAPP/NF(N-Me)GA(N-Me)IL incubations, assay buffer solution containing NF(N-Me)GA(N-Me)IL was added to hIAPP. For the 1:10 hIAPP/NF(N-Me)GA(N-Me)IL incubations, reproducible results were obtained when NF(N-Me)GA(N-Me)IL was first mixed with hIAPP in HFIP and, after evaporation of the HFIP, the remaining film-like pellet was then diluted into the assay buffer. Incubations in assay buffer with 1%–2% HFIP were performed to study the effect of the inhibitor on a prenucleated system [14]. In preliminary experiments, we found that the fluorescence emission of ThT bound to hIAPP fibrils was proportional to amyloid fibril concentration.

Analysis of the Composition of Precipitated Aggregates

After peptide precipitation in a CD experiment, the suspension (800 μl) was centrifuged (12,000 × g; 10 min), and the pellet redissolved in 100 μl DMSO and injected onto a Nucleosil 100 C-18 semipreparative column (Grom, Herrenberg, Germany) (100 Å pore size, 7 μm paricle size, 8 × 250 mm). Supernatants were also analyzed by RP-HPLC. Eluents and flow rates were as previously described [29], and the peptides were identified by their retention times.

Assessment of Cell Viability with the MTT Reduction Assay

The rat insulinoma cell line RIN 5fm was obtained by T.E. Rucinsky from the Washington University Tissue Culture Support Center, and cells were cultured as described [29]. Cells were plated in 96-well plates at a density of 5 × 10^5 cells/ml (100 μl/well) [29]. After incubation for 24 hr (37°C, humidified atmosphere with 5% CO_2), serial dilutions of a seedless hIAPP solution (5 μM, in 10 mM sodium phosphate buffer [pH 7.4] [assay buffer]) or solutions containing a mixture of seedless hIAPP (5 μM) with NF(N-Me)GA(N-Me)IL, NFGAIL, PrP(117-122), or (N-Me)IAF(N-Me)GNL (at 50 μM or 500 nM) were applied to the cells. After incubation for 20 hr, cell viability was assessed by measuring the cellular reduction of MTT as described [29, 43]. In all studies, a dose-response curve of hIAPP alone was obtained in parallel to the mixture curves to control for differences in hIAPP cytotoxicity because of variations in its aggregation states. The incubations that were made to study the effect of NFGAIL on hIAPP cytotoxicity (Figure 5B) contained 1% HFIP because of the low solubility of NFGAIL. We obtained more reproducible results in the hIAPP/peptide incubations at a 1:10 molar ratio when the peptides were first mixed with hIAPP in HFIP and, after evaporation of the HFIP, the remaining pellet was then diluted into the assay buffer.

Assessment of Apoptosis

Cells (see above) were platted in 12-well plates at a density of 5 × 10^5 cells/ml (750 μl/well). After incubation for 24 hr (37°C, humidified atmosphere with 5% CO_2), hIAPP (5 μM, in 10 mM sodium phosphate buffer [pH 7.4]) or a solution containing a mixture of hIAPP (5 μM) with NF(N-Me)GA(N-Me)IL (500 nM) or vehicle alone were applied to the cells at a peptide final concentration of 500 nM hIAPP alone or 500 nM hIAPP and 50 nM NF(N-Me)GA(N-Me)IL. After incubation for 20 hr (37°C, humidified atmosphere with 5% CO_2), cells were detached from the wells by treatment with a trypsin/EDTA solution and counted, and apoptosis was assessed by the Cell Death Detection ELISA kit (Roche Diagnostics, Mannheim, Germany).

Binding of NF(N-Me)GA(N-Me)IL to Soluble, Fluorescein-Labeled hIAPP

Fluorescence measurements were performed on a Spex Fluorolog 2 fluorescence spectrophotometer with a 1 cm path-length cuvette. Excitation was at 492 nm, and fluorescence emission spectra between 500 and 600 nm were recorded. The exact concentration of Fluos-hIAPP (freshly made stock solution in HFIP) was determined by UV spectroscopy. All fluorescence measurements were performed in 10 mM sodium phosphate buffer (pH 7.4) containing 1% HFIP at room temperature within the first 2–5 min after solution preparation. Both hIAPP and NF(N-Me)GA(N-Me)IL or the control peptides were added to the aqueous buffer solution from suitable stock solutions in HFIP. In Figure 6B, the maximum fluorescence intensities of various mixtures of Fluos-hIAPP and NF(N-Me)GA (N-Me)IL at 522 nm (after subtraction of the fluorescence of Fluos-hIAPP) were plotted versus the logarithm of free NF(N-Me)GA (N-Me)IL concentration. Because the concentration of Fluos-hIAPP is more than 100-fold lower than the apparent K_d of the complex, the concentration of added NF(N-Me)GA(N-Me)IL was assumed to be approximately the same as the concentration of free NF(N-Me) GA(N-Me)IL [58]. Sigmoidal curve fitting and determination of the apparent K_d were performed with GraphPad Prism software using the following equation: $F = F_0 + [(F_{sat} - F_0) / (1 + 10^{(LogKd-L).HillSlope})]$ in which F is the observed fluorescence intensity, F_0 is the fluorescence of Fluos-hIAPP alone, F_{sat} is the fluorescence intensity at saturation, L is the logarithm of the concentration of NF(N-Me) GA(N-Me)IL, and K_d is the apparent dissociation constant [60, 68].

Studying the Binding of Fluorescein-Labeled Peptides to Deposits of Human Pancreatic Amyloid and Canine Renal AA Amyloid

Human pancreatic tissue with islet amyloid obtained postmortem and canine renal tissue with reactive (AA) amyloidosis were stored frozen at –20°C. Frozen sections (10 μm) were mounted on glass slides and fixed in ice-cold acetone for 10 min and rinsed five times in 10 mM sodium phosphate buffer with 0.15 sodium cloride (PBS) (pH 7.4). Sections were incubated with fluorescently labeled peptides NF(N-Me)GA(N-Me)IL, NFGAIL, or hIAPP(1–13) (10 μM in PBS). Incubation took place in a humidity chamber at room temperature for 12 hr. After incubation, the sections were rinsed in PBS and mounted with Vectashield mounting medium (Vector laboratories, Burlingame, CA). Consecutive sections were stained for amyloid with Congo red [50, 64]. Fluorescent staining was studied on a Nikon eclipse E800 microscope equipped with an excitation filter at 450 nm for detection of fluorescein fluorescence and an excitation filter at 546 nm for detection of Congo red fluorescence [50, 64].

Acknowledgments

We are grateful to J. Bernhagen for help with the apoptosis assay and to A. Velkova for help with the fluorescence spectroscopy. We thank K. Sweimeh for technical assistance in CD and EM studies. We thank M. Waldner, H. Vasan, and M. Müsken for technical assistance in peptide synthesis, purification, and fluorescein labeling. This work was partially supported by an institutional grant of The Fraunhofer Institute for Interfacial and Biological Engineering (FhIGB, Stuttgart, Germany).

Received: November 17, 2004
Revised: March 26, 2005
Accepted: May 9, 2005
Published: July 22, 2005

References

1. Hull, R.L., Westermark, G.T., Westermark, P., and Kahn, S.E. (2004). Islet amyloid: a critical entity in the pathogenesis of type 2 diabetes. J. Clin. Endocrinol. Metab. *89*, 3629–3643.
2. Ahmed, S., Clark, A., and Matthews, D.R. (1997). Progressive decline of β-cell function in non-insulin dependent diabetes. Curr. Opin. Endocrinol. Diabetes *4*, 300–307.
3. Opie, E.L. (1901). On the relation of chronic interstitial pancreatitis to the islands of Langerhans and to diabetes mellitus. J. Exp. Med. *5*, 397–428.
4. Westermark, P., Wernstedt, C., Wilander, E., Hayden, D.W., O'Brien, T.D., and Johnson, K.H. (1987). Amyloid fibrils in human insulinoma and islets of Langerhans of the diabetic cat are derived from a neuropeptide-like protein also present in normal islet cells. Proc. Natl. Acad. Sci. USA *84*, 3881–3885.
5. Wimalawansa, S.J. (1997). Amylin, calcitonin gene-related peptide, calcitonin, and adrenomedullin: a peptide superfamily. Crit. Rev. Neurobiol. *11*, 167–239.
6. Nyholm, B., Finernan, M.S., Koda, J.E., and Schmitz, O. (1998). Plasma amylin immunoreactivtiy and insulin resistance in insulin resistant relatives of patients with non-insulin-dependent diabetes mellitus. Horm. Metab. Res. *30*, 206–212.
7. Lorenzo, A., Razzboni, B., Weir, G.C., and Yankner, B.A. (1994). Pancreatic islet cell toxicity of amylin associated with type-2 diabetes mellitus. Nature *368*, 756–760.
8. Kapurniotu, A. (2001). Amyloidogenicity and cytotoxicity of islet amyloid polypeptide. Biopolymers *60*, 438–459.
9. Janson, J., Ashley, R.H., Harrison, D., McIntyre, S., and Butler, P.C. (1999). The mechanism of islet amyloid polypeptide toxicity is membrane disruption by intermediate-sized toxic amyloid particles. Diabetes *48*, 491–498.
10. Anguiano, M., Nowak, R., and Lansbury, P.T.J. (2002). Protofibrillar islet amyloid polypeptide permeabilizes synthetic vesicles by a pore-like mechanism that may be relevant to type II diabetes. Biochemistry *41*, 11338–11343.
11. Porat, Y., Kolusheva, S., Jelinek, R., and Gazit, E. (2003). The

human islet amyloid polypeptide forms transient membrane-active prefibrillar assemblies. Biochemistry *42*, 10971–10977.
12. Green, J.D., Goldsbury, C., Kistler, J., Cooper, G.J., and Aebi, U. (2004). Human amylin oligomer growth and fibril elongation define two distinct phases in amyloid formation. J. Biol. Chem. *279*, 12206–12212.
13. Kayed, R., Bernhagen, J., Greenfield, N., Sweimeh, K., Brunner, H., Voelter, W., and Kapurniotu, A. (1999). Conformational transitions of islet amyloid polypeptide (IAPP) in amyloid formation *in vitro*. J. Mol. Biol. *287*, 781–796.
14. Padrick, S.B., and Miranker, A.D. (2002). Islet amyloid: phase partitioning and secondary nucleation are central to the mechanism of fibrillogenesis. Biochemistry *41*, 4694–4703.
15. Lorenzo, A., and Yankner, B.A. (1994). β-amyloid neurotoxicity requires fibril formation and is inhibited by congo red. Proc. Natl. Acad. Sci. USA *91*, 12243–12247.
16. Tomiyama, T., Kaneko, H., Kataoka, K., Asano, S., and Endo, N. (1997). Rifampicin inhibits the toxicity of pre-aggregated amyloid peptides by binding to peptide fibrils and preventing amyloid-cell interaction. Biochem. J. *322*, 859–865.
17. Kudva, Y.C., Mueske, C., Butler, P.C., and Eberhardt, N.L. (1998). A novel assay in vitro of human islet amyloid polypeptide amyloidogenesis and effects of insulin secretory vesicle peptides on amyloid formation. Biochem. J. *331*, 809–813.
18. Aitken, J.F., Loomes, K.M., Konarkowska, B., and Cooper, G.J.S. (2003). Suppression by polycyclic compounds of the conversion of human amylin into insoluble amyloid. Biochem. J. *374*, 779–784.
19. Harroun, T.A., Bradshaw, J.P., and Ashley, R.H. (2001). Inhibitors can arrest the membrane activity of human islet amyloid polypeptide independently of amyloid formation. FEBS Lett. *507*, 200–204.
20. Scrocchi, L.A., Chen, Y., Waschuk, S., Wang, F., Cheung, S., Darabie, A.A., McLaurin, J., and Fraser, P.E. (2002). Design of peptide-based inhibitors of human islet amyloid polypeptide fibrillogenesis. J. Mol. Biol. *318*, 697–706.
21. Gilead, S., and Gazit, E. (2004). Inhibition of amyloid formation by peptide analogues modified with α-aminoisobutyric acid. Angew. Chem. Int. Ed. Engl. *43*, 4041–4044.
22. Kapurniotu, A., Schmauder, A., and Tenidis, K. (2002). Structure-based design and study of non-amyloidogenic, double N-methylated IAPP amyloid core sequences as inhibitors of IAPP amyloid formation and cytotoxicity. J. Mol. Biol. *315*, 339–350.
23. Rajarathnam, K., Clark-Lewis, I., and Sykes, B.D. (1995). 1H NMR solution structure of an active monomeric interleukin-8. Biochemistry *34*, 12983–12990.
24. Sun, X., and Lorenzi, G.P. (1994). On the stacking of β-rings: the solution self-association behavior of two partially N-methylated cyclo(hexaleucines). Helv. Chim. Acta *77*, 1520–1526.
25. Chitnumsub, P., Fiori, W.R., Lashuel, H.A., Diaz, H., and Kelly, J.W. (1999). The nucleation of monomeric parallel β-sheet-like structures and their self-assambly in aqueous solution. Bioorg. Med. Chem. *7*, 39–59.
26. Sagan, S., Karoyan, P., Lequin, O., Chassaing, G., and Laviell, S. (2004). N- and Cα-methylation in biologically active peptides: synthesis, structural and functional aspects. Curr. Med. Chem. *11*, 2799–2822.
27. Gordon, D.J., Sciarretta, K.L., and Meredith, S.C. (2001). Inhibition of β-amyloid(40) fibrillogenesis and disassembly of β-amyloid(40) fibrils by short β-amyloid congeners containing N-methyl amino acids at alternate residues. Biochemistry *40*, 8237–8245.
28. Hughes, E., Burke, R.M., and Doig, A.J. (2000). Inhibition of toxicity in the β-amyloid peptide fragment β-(25-35) using N-methylated derivatives. J. Biol. Chem. *275*, 25109–25115.
29. Tenidis, K., Waldner, M., Bernhagen, J., Fischle, W., Bergmann, M., Weber, M., Merkle, M.-L., Voelter, W., Brunner, H., and Kapurniotu, A. (2000). Identification of a penta- and hexapeptide of islet amyloid polypeptide (IAPP) with amyloidogenic and cytotoxic properties. J. Mol. Biol. *295*, 1055–1071.
30. Zanuy, D., Ma, B., and Nussinov, R. (2003). Short peptide amyloid organization: stabilities and conformations of the islet amyloid polypeptide NFGAIL. Biophys. J. *84*, 1884–1894.
31. Zanuy, D., Porat, Y., Gazit, E., and Nussinov, R. (2004). Peptide sequence and amyloid formation; molecular simulations and experimental study of a human islet amyloid polypeptide fragment and its analogs. Structure *12*, 439–455.
32. Griffiths, J.M., Ashburn, T.T., Auger, M., Costa, P., Griffin, R.G., and Lansbury, P.T.J. (1995). Rotational resonance solid-state NMR elucidates a structural model of pancreatic amyloid. J. Am. Chem. Soc. *117*, 3539–3546.
33. Kapurniotu, A., Bernhagen, J., Greenfield, N., Al-Abed, Y., Teichberg, S., Frank, R.W., Voelter, W., and Bucala, R. (1998). Contribution of advanced glycosylation to the amyloidogenicity of islet amyloid polypeptide. Eur. J. Biochem. *251*, 208–216.
34. Jarrett, J.T., and Lansbury, P.T., Jr. (1993). Seeding one-dimensional crystallization of amyloid: a pathogenic mechanism in Alzheimer's disease and scrapie? Cell *73*, 1055–1058.
35. Woody, R.W. (1985). Circular dichroism of peptides. In The Peptides: Analysis, Synthesis, Biology, S. Udenfriend, J. Meienhofer, and V. Hruby, eds. (New York: Academic Press), pp. 15–114.
36. Goldsbury, C., Goldie, K., Pellaud, J., Seelig, J., Frey, P., Müller, S.A., Kistler, J., Cooper, G.J.S., and Aebi, U. (2000). Amyloid fibril formation from full-length and fragments of amylin. J. Struct. Biol. *130*, 352–362.
37. Moriarty, D.F., and Raleigh, D.P. (1999). Effects of sequential proline substitutions on amyloid formation by human amylin20-29. Biochemistry *38*, 1811–1818.
38. Westermark, P., Engström, U., Johnson, K., Westermark, G.T., and Betsholz, C. (1990). Islet amyloid polypeptide: pinpointing amino acid residues linked to amyloid fibril formation. Proc. Natl. Acad. Sci. USA *87*, 5036–5040.
39. LeVine, H., 3rd. (1999). Quantification of β-sheet amyloid fibril structures with thioflavin T. In Methods in Enzymology: Amyloid, Prions, and Other Protein Aggregates, R. Wetzel, ed. (New York: Academic Press), pp. 274–284.
40. LeVine, H., 3rd. (1993). Thioflavine T interaction with synthetic Alzheimer's disease β-amyloid peptides: detection of amyloid aggregation in solution. Protein Sci. *2*, 404–410.
41. Padrick, S.B., and Miranker, A.D. (2001). Islet amyloid polypeptide: identification of long-range contacts and local order on the fibrillogenesis pathway. J. Mol. Biol. *308*, 783–794.
42. Shearman, M.S., Hawtin, S.R., and Tailor, V.J. (1995). The intracellular component of cellular 3-(4,5-dimethythiazol-2-yl)-2,5-Diphenyltetrazolium bromide (MTT) reduction is specifically inhibited by β-amyloid peptides. J. Neurochem. *65*, 218–227.
43. Shearman, M.S., Ragan, C.I., and Iversen, L.L. (1994). Inhibition of PC12 cell redox activity is a specific, early indicator of the mechanism of β-amyloid-mediated cell death. Proc. Natl. Acad. Sci. USA *91*, 1470–1474.
44. Schubert, D., Behl, C., Lesley, R., Brack, A., Dargusch, R., Sagara, Y., and Kimura, H. (1995). Amyloid peptides are toxic via a common oxidative mechanism. Proc. Natl. Acad. Sci. USA *92*, 1989–1993.
45. Kapurniotu, A., Buck, A., Weber, M., Schmauder, A., Hirsch, T., Bernhagen, J., and Tatarek-Nossol, M. (2003). Conformational restriction via cyclization in β-amyloid peptide Aβ(1-28) leads to an inhibitor of Aβ(1-28) amyloidogenesis and cytotoxicity. Chem. Biol. *10*, 149–159.
46. Saafi, E.L., Konarkowska, B., Zhang, S., Kistler, J., and Cooper, G. (2001). Ultrastructural evidence that apoptosis is the mechanism by which human amylin evokes death in RINm5F pancreatic beta-cells. Cell Biol. Int. *25*, 339–350.
47. Zhang, S., Liu, J., MacGibbon, G., Dragunow, M., and Cooper, G.J.S. (2002). Increased expression and activation of c-Jun contributes to human amylin induced apoptosis in pancreatic islet β-cells. J. Mol. Biol. *324*, 271–285.
48. Duke, R.C., and Cohen, J.J. (1986). IL-2 addiction: withdrawal of growth factor activates a suicide program in dependent T cells. Lymphokine Res. *5*, 289–299.
49. Corsaro, A., Thellung, S., Villa, V., Principe, D.R., Paludi, D., Arena, S., Millo, E., Schettini, D., Damonte, G., Aceto, A., et al. (2003). Prion protein fragment 106-126 induces a p38 MAP kinase-dependent apoptosis in SH-SY5Y neuroblastoma cells independently from the amyloid fibril formation. Ann. N Y Acad. Sci. *1010*, 610–622.

50. Puchtler, H., and Sweat, F. (1965). Congo red as a stain for fluorescence microscopy of amyloid. J. Histochem. Cytochem. *13*, 693–694.
51. Cooper, J.H. (1974). Selective amyloid staining as a function of amyloid composition and structure. Lab. Invest. *31*, 232–238.
52. Gazit, E. (2002). Mechanistic studies of the process of amyloid fibrils formation by the use of peptide fragments and analogues: implications for the design of fibrillization inhibitors. Curr. Med. Chem. *9*, 1725–1735.
53. Mazor, Y., Gilead, S., Benhar, I., and Gazit, E. (2002). Identification and characterization of a novel molecular-recognition and self-assembly domain within the islet amyloid polypeptide. J. Mol. Biol. *322*, 1013–1024.
54. Azriel, R., and Gazit, E. (2001). Analysis of the minimal amyloid-forming fragment of the islet amyloid polypeptide. J. Biol. Chem. *276*, 34156–34161.
55. Manning, M.C., Illangasekare, M., and Woody, R.W. (1988). Circular dichroism studies of distorted α-helices, twisted β-sheets, and β-turns. Biophys. Chem. *31*, 77–86.
56. Gordon, D.J., Tappe, R., and Meredith, S.C. (2002). Design and characterization of a membrane permeable N-methyl amino acid-containing peptide that inhibits Ab1-40 fibrillogenesis. J. Pept. Res. *2002*, 37–55.
57. LeVine, H., 3rd, and Scholten, J.D. (1999). Screening for pharmacological inhibitors of amyloid fibril formation. In Methods of Enzymology: Amyloid, Prions, and Other Protein Aggregates, R. Wetzel, ed. (New York: Academic Press), pp. 467–476.
58. Eftink, M.R. (1997). Fluorescence methods for studying equilibrium macromolecule-ligand interactions. In Methods in Enzymology: Fluorescence Spectroscopy, L. Brand and M.L. Johnson, eds. (New York: Academic Press), pp. 221–257.
59. Tjerberg, L.O., Pramanik, A., Björling, S., Thyberg, P., Thyberg, J., Nordstedt, C., Berndt, K.D., Terenious, L., and Rigler, R. (1999). Amyloid β-peptide polymerization studied using fluorescence correlation spectroscopy. Chem. Biol. *6*, 53–62.
60. Maroun, R.G., Gayet, S., Benleulmi, M.S., Porumb, H., Zargarian, L., Merad, H., Leh, H., Mouscadet, J.F., Troalen, F., and Fermandjian, S. (2001). Peptide inhibitors of HIV-1 integrase dissociate the enzyme oligomers. Biochemistry *40*, 13840–13848.
61. Mirzabekov, T.A., Lin, M., and Kagan, B.L. (1996). Pore formation by the cytotoxic islet amyloid peptide amylin. J. Biol. Chem. *271*, 1988–1992.
62. Ross, C.A., and Poirier, M.A. (2004). Protein aggregation and neurodegenerative disease. Nat. Med. Suppl. *10*, 10–17.
63. Tomiyama, T., Shoji, A., Kataoka, K., Suwa, Y., Asano, S., Kaneko, H., and Endo, N. (1996). Inhibition of amyloid β protein aggregation and neurotoxicity by rifampicin. J. Biol. Chem. *271*, 6839–6844.
64. Westermark, G.T., Johnson, K.H., and Westermark, P. (1999). Staining methods for identification of amyloid in tissue. In Methods in Enzymology: Amyloid, Prions, and Other Protein Aggregates, R. Wetzel, ed. (New York: Academic Press), pp. 3–25.
65. Adessi, C., Frossard, M.J., Boissard, C., Fraga, S., Bieler, S., Ruckle, T., Vilbois, F., Robinson, S.M., Mutter, M., Banks, W.A., et al. (2003). Pharmacological profiles of peptide drug candidates for the treatment of Alzheimer's disease. J. Biol. Chem. *278*, 13905–13911.
66. Wiesehan, K., Buder, K., Linke, R.P., Patt, S., Stoldt, M., Unger, E., Schmitt, B., Bucci, E., and Willbold, D. (2003). Selection of D-amino-acid peptides that bind to Alzheimer's disease amyloid peptide abeta1-42 by mirror image phage display. ChemBioChem *4*, 748–753.
67. Kapurniotu, A., Kayed, R., Taylor, J.W., and Voelter, W. (1999). Rational design, confomational studies and bioactivity of novel, highly potent, conformationally constrained calcitonin analogues. Eur. J. Biochem. *265*, 606–618.
68. Lim, W.A., Fox, R.O., and Richards, F.M. (1994). Stability and peptide binding affinity of an SH3 domain from the *Caenorhabditis elegans* signaling protein Sem-5. Protein Sci. *3*, 1261–1266.